J. Pineal Res. 2008; 45:157–165
Doi:10.1111/j.1600-079X.2008.00570.x

Journal of Pineal Research

Melatonin impairs NADPH oxidase assembly and decreases superoxide anion production in microglia exposed to amyloid-β_{1-42}

Abstract: Melatonin shows significant protective effects in Alzheimer's disease (AD) models in vitro and in vivo; these effects are related to its function as an antioxidant. The source of reactive oxygen species (ROS) generation in the AD brain is primarily the amyloid-β (Aβ)- activated microglial nicotinamide adenine dinucleotide phosphate (NADPH) oxidase. However, the effects of melatonin on the activation of NADPH oxidase remain unclear. In the present study, the cultures of microglia were incubated in the presence of fibrillar Aβ_{1-42}, which induces the assembly and the activation of NADPH oxidase, and triggers the production of superoxide anion-derived ROS. Pretreatment of microglia with melatonin dose-dependently prevents the activation of NADPH oxidase and decreases the production of ROS. Melatonin inhibits the phosphorylation of the $p47^{phox}$ subunit of NADPH oxidase via a PI3K/Akt-dependent signalling pathway, blocks the translocation of $p47^{phox}$ and $p67^{phox}$ subunit to the membrane, down-regulates the binding of $p47^{phox}$ to $gp91^{phox}$, and impairs the assembly of NADPH oxidase. Our data offer new insights into the mechanism of inhibiting ROS generation by melatonin in Aβ-activated microglia. Inhibition of ROS production indirectly might be the underlying mechanism for the neuroprotection by melatonin in the AD brain.

Juefei Zhou[1,2,*], Shen Zhang[3,*], Xingyu Zhao[1,2] and Taotao Wei[1]

[1]National Laboratory of Biomacromolecules, Institute of Biophysics, Chinese Academy of Science, Beijing; [2]Graduate University of Chinese Academy of Science, Beijing; [3]Department of Laboratory Medicine, Huaihua Medical College, Huaihua, China

Key words: Alzheimer's disease, amyloid-β, melatonin, microglia, NADPH oxidase, superoxide anion

Address reprint requests to Taotao Wei, National Laboratory of Biomacromolecules, Institute of Biophysics, Chinese Academy of Sciences, 15 Datun Road, Chaoyang District, Beijing 100101, China
E-mail: weitt@moon.ibp.ac.cn

*J Zhou and S Zhang contributed equally to this work.

Received November 1, 2007;
accepted January 14, 2008.

Introduction

Melatonin (*N*-acetyl-5-methoxytryptamine) is secreted mainly, but not exclusively by the pineal gland [1]. Other organs and tissues including retina, gut, ovary, testes, bone marrow and lens have been reported to produce melatonin as well [2]. Once formed melatonin is not stored within the pineal gland but diffuses out into the capillary blood [3] and cerebrospinal fluid (CSF) [4]. Available data regarding melatonin concentrations in tissues, cells or other body fluids are variable and range from picomolar to micromolar levels, which presumably change in a circadian manner. Levels of melatonin released to the CSF were found to be 5 to 10 (up to 30) times higher than those simultaneously measured in the blood [4]. Based on previous reports, it seems that the brain tissue may have higher melatonin levels than other tissues in the body [5].

The biological functions of melatonin have been investigated extensively. Melatonin controls important physiological functions including seasonal reproduction and circadian rhythms. Moreover, melatonin and its metabolites show potent antioxidant capacities in vitro and in vivo, and they scavenge both hydrophilic and hydrophobic reactive oxygen species (ROS) [6–9]. They protect biomacromolecules from oxidative damage [10, 11]. Also, the molecules protect neurons from various degenerative disorders involving free radical generation. These disorders include Alzheimer's disease (AD) [12–14], Parkinson's disease [15, 16] and ischaemia-reperfusion neuronal injury [17].

Alzheimer's disease is the most common neurodegenerative disease known to cause dementia in the elderly, and manifests as progressive cognitive decline and profound neuronal loss. AD is clinically associated with cognitive impairment, loss of language and motor skills, and changes in behaviour. The principal neuropathological hallmarks of AD are the extracellular plaques of amyloid-β (Aβ), the intracellular neurofibrillary tangles (NFTs), and loss of synaptic connections within entorhinal cortex and progressing into the hippocampus and cortex [18–20]. Although melatonin shows significant protective effects in AD models in vitro and in vivo [12–14], the underlying mechanisms remain unclear. It is hypothesized that the protective effects of melatonin are related to its function as an antioxidant. In the AD brain, the source of ROS generation is primarily the Aβ-activated microglial nicotinamide adenine dinucleotide phosphate (NADPH) oxidase [21]. The NADPH oxidase plays an essential role in innate immune system. NADPH oxidase is found associated with plasma membranes where it can release superoxide anion. This released superoxide serves as a precursor for additional ROS, including

hydrogen peroxide, hydroxyl radical, peroxynitrite and other oxidants that aid in the killing of the pathogen. Excessive production of ROS by microglial NADPH oxidase is cytotoxic and can damage neurons adjacent to sites of inflammatory action. As the neuroprotective effects of melatonin are related to its antioxidant properties, we used as a working hypothesis that melatonin might eliminate NADPH oxidase-derived ROS.

In the present study the cultures of microglia were incubated in the presence of fibrillar Aβ, and the effects of melatonin on ROS (superoxide and superoxide-derived ROS) generation and NADPH oxidase assembly were investigated. The underlying mechanisms were also discussed.

Materials and methods

Chemicals and antibodies

Dulbecco's modifed Eagle medium (DMEM), foetal bovine serum and cell culture supplements were obtained from Hyclone (Logan, UT, USA). 2′,7′-Dichlorofluorescin diacetate (DCFH-DA) and the NADPH oxidase inhibitor diphenylene iodonium (DPI) were from Molecular Probes (Eugene, OR, USA). Manganese (III) tetrakis(1-methyl-pyridy)porphyrin pentachloride (MnTMPyP) and the Akt inhibitor 1L-6-hydroxymethyl-chiro-inositol 2-(R)-2-O-methyl-3-O-octadecylcarbonate were purchased from Calbiochem (La Jolla, CA, USA). The PI3K inhibitors wortmannin and LY294002 were from Alexis Biochemicals (San Diego, CA, USA). Melatonin, 5,5-dimethyl-1-pyrroline-*N*-oxide (DMPO), hypoxanthine, xanthine oxidase and amyloid-β_{1-42} were products of Sigma (St Louis, MO, USA). Goat polyclonal antibodies against NADPH oxidase subunits ($p22^{phox}$, $p47^{phox}$, $p67^{phox}$ and $gp91^{phox}$) were purchased from Santa Cruz Biotechnology (Santa Cruz, CA, USA). Monoclonal antibodies against phospho-Akt and total Akt were from Cell Signaling (Beverly, CA, USA). Rabbit antiphosphoserine antibody was purchased from Invitrogen (Shanghai, China).

Cell culture

Primary cultures of rat mixed glia were prepared from the cerebral cortices of neonatal Sprague-Dawley rats (Beijing Vital River Experimental Animal Center, Beijing City, China) with protocols we described previously [22]. Briefly, cerebral cortices from six neonatal rats were dissected and freed of meninges. Cells were dissociated by mild trypsinization, followed by triturating and passing through a nylon mesh. Cells (2×10^7) were plated in 75 cm^2 culture flasks in 20 mL culture medium consisted of DMEM supplemented with 10% foetal bovine serum, 2 mM L-glutamine, 100 U/mL penicillin and 100 μg/mL streptomycin. Cultures were kept at 37°C in a humidified incubator gassed with 5% CO_2 and air. At the 12th to 14th day in vitro, confluent cultures of mixed glia were shaken for 3 hr at 180 rpm in a rotary shaker to separate microglia. Detached microglia were plated on 60 mm culture dishes, 100 mm culture dishes or 96-well microplates at a density of 2×10^5 cells per cm^2, and cultured for additional 24 hr.

Treatment of microglia with amyloid-β_{1-42}

Amyloid-β_{1-42} was solubilized and then aggregated in insoluble fibrils as described previously [12]. Briefly, 100 μM of Aβ in phosphate-buffered saline (PBS) was allowed to incubate under agitation (Teflon stir bar at 800 rpm) at 23°C for 36 hr. After centrifugation (15,000 × g; 10 min), the pellet was resuspended in DMEM to form a 100 μM stock solution of insoluble amyloid-β_{1-42} fibrils. Melatonin stock solution (1 M) was prepared in DMSO and stored at −20°C.

The microglia were exposed to insoluble amyloid-β_{1-42} fibrils by adding the stock solution of Aβ to the wells (final concentration: 5 or 20 μM). In some experiments, microglia were preincubated with melatonin (final concentration: 10, 50 or 100 μM) for 30 min before the addition of Aβ. Incubation of microglia with Aβ (up to 30 μM) or melatonin (up to 200 μM) did not influence the viability of microglia, as assessed by trypan blue exclusion (data not shown).

Assay of ROS

The levels of intracellular ROS were determined with a fluorescence microplate reader using DCFH-DA as a ROS-sensitive fluorescence probe [23]. DCFH-DA is a nonfluorescent compound that can permeate cells freely. When inside cells, DCFH-DA is cleaved by endogenous esterases to form DCFH and is trapped inside cells. Upon oxidation by the cytosolic ROS, it is converted to the fluorescent compound 2′,7′-dichlorofluorescein (DCF) and the fluorescent signal detected is proportional to ROS production.

Microglia grown on 96-well microplate were exposed to Aβ for indicated intervals and then loaded with 20 μM DCFH-DA and incubated for additional 1 hr. The fluorescent signal of DCF was detected with Fluoroskan Ascent microplate reader with excitation wavelength 485 nm and emission wavelength 538 nm. In order to determine whether the increase in DCF fluorescence is a result of NADPH oxidase activity, some of the wells were pretreated with the NADPH oxidase inhibitor diphenyleneiodonium (DPI, 2 and 5 μM) for 30 min before the addition of Aβ. The influence of PI3K inhibitors (wortmannin, 100 nM; and LY294002, 50 μM), Akt inhibitor (1L-6-hydroxymethyl-chiro-inositol 2-(R)-2-O-methyl-3-O-octadecylcarbonate, 5 and 10 μM), and superoxide anion scavenger manganese (III) tetrakis(1-methyl-pyridy)porphyrin pentachloride (MnTMPyP, 10 and 25 μM) on the cellular ROS levels were also studied by pretreating cells with these drugs for 30 min before the addition of Aβ.

EPR studies

The production of superoxide anion in Aβ-activated microglia was detected directly by EPR spin trapping technique, using 5,5-dimethyl-1-pyrroline-N-oxide (DMPO) as the spin trap [24]. Briefly, microglia grown on 100 mm dishes were exposed to Aβ for 12 hr. Cells were collected with a rubber policeman and suspended in 100 μL of Hank's balanced salt solution (HBSS) containing 0.1 M of the spin trap DMPO, transferred into quartz capillary

and fitted into the cavity of Bruker ER-200 D-SRC EPR spectrometer (Bruker-Biospin, Rheinstetten, Germany). After incubation at 37°C for 2 min, the EPR spectrum was recorded immediately with conditions described as follows: X-band; sweep width 200 G; microwave power 20 mW; 100 kHz modulation with amplitude 1 G; time constant 0.128 s.

The direct scavenging of superoxide anion by melatonin was also studied by EPR spectrometry according to method we reported previously [25]. Briefly, superoxide radicals were generated with hypoxanthine and xanthine oxidase. Reaction mixtures containing 0.5 mM hypoxanthine, 0.96 mM DETAPAC, 0.1 M DMPO and different concentrations of melatonin were premixed, after the addition of 0.05 U/mL xanthine oxidase, the reaction mixtures were transferred into quartz capilaries for ESR measurement. The ESR spectra were recorded 40 s after the addition of xanthine oxidase.

Mobilization of p47^{phox} and p67^{phox} subunits to plasma membrane

Translocation to membrane of p47^{phox} and p67^{phox} NADPH oxidase subunits was analysed by Western blot, as previously reported [26], with minor modifications, and the membrane levels of the p22^{phox} subunit were monitored as a control. Briefly, microglia cultured on 60 mm dishes were exposed to Aβ for indicated intervals and harvested with a rubber policeman. Cells were suspended in 200 μL ice-cold buffer consisting of 10 mM Tris–HCl (pH 7.3), 100 mM KCl, 3 mM NaCl, 3.5 mM $MgCl_2$, 1.25 mM EGTA, 1 mM ATP, 2 mM Na_3VO_4, 100 μM phenylarsine oxide, 3 mM diisopropyl fluorophosphate, 10 μg/mL leupeptin, and 10 μg/mL aprotinin, and disrupted by sonication on ice. After ultracentrifugation at 100,000 × g for 30 min at 4°C, the membrane pellet obtained was resuspended in solubilization buffer consisting of 10 mM Tris–HCl (pH 7.4), 150 mM NaCl, 5 mM EDTA, 1% sodium deoxycholate, 1% Nonidet-P40, and 0.1% SDS, and then recentrifuged at 20,000 × g for 40 min at 4°C. The supernatant containing solubilized membrane proteins were separated on a 10% sodium dodecyl sulfate-polyacrylamide gel electrophoresis (SDS-PAGE) and then electroblotted onto PVDF membrane. The membrane was probed with antibodies against p67^{phox}, p47^{phox} and p22^{phox}, respectively, and then incubated with horseradish peroxidase-conjugated second antibodies. After four washes with 0.05% tris buffered salt solution containing 0.5% Tween-20 (TBST), the target proteins were detected by using an enhanced chemiluminescence assay.

Immunoprecipitation

Microglia cultured on 100 mm dishes were exposed to Aβ for indicated intervals, harvested with a rubber policeman, and lysed in 1 mL buffer consisting of 10 mM Tris–HCl (pH 7.4), 150 mM NaCl, 5 mM EDTA, 1% Triton X-100, 10 mM NaF, 1 mM Na_3VO_4, 10 μg/mL leupeptin, 10 μg/mL aprotinin and 20 mM PMSF. Aliquots of the cellular lysates (containing 500 μg protein) were incubated with proper primary antibodies (anti-p47^{phox} and anti-Akt1 antibodies) with rocking for overnight at 4°C. Protein was then immunoprecipitated using Amersham Pharmacia gamma-bind G-Sepharose beads.

Detection of phosphorylated p47^{phox} and the binding of p47^{phox}–gp91^{phox}

The immunoprecipitated proteins with anti-p47^{phox} antibody were separated on a 10% SDS-PAGE gel and were then electroblotted onto PVDF membrane. The membranes were probed with anti-phosphoserine antibody, anti-gp91^{phox} antibody or anti-p47^{phox} antibody, to detect the phosphorylation of p47^{phox}, the binding of p47^{phox}–gp91^{phox}, or total amount of p47^{phox}, respectively. After incubation with horseradish peroxidase-conjugated second antibodies and four washes with 0.05% TBST, the target proteins were detected by using an enhanced chemiluminescence assay.

Detection of Akt activation

Phosphorylation of Akt was analysed by Western blot analysis using an anti-phospho-Akt-1 antibody and the total Akt was analysed with an anti-Akt1 antibody. Briefly, microglia grown on 60 mm dishes were pretreated with or without drugs, incubated with Aβ for indicated intervals, harvested with a rubber policeman and lysed in 200 μL buffer consisting of 10 mM Tris–HCl (pH 7.4), 150 mM NaCl, 5 mM EDTA, 1% Triton X-100, 10 mM NaF, 1 mM Na_3VO_4, 10 μg/mL leupeptin, 10 μg/mL aprotinin and 20 mM PMSF. Proteins were separated on a 10% SDS-PAGE, electroblotted onto PVDF membranes, and probed with antibodies against phosphor-Akt1 or total Akt1, respectively. The target proteins were detected by using an enhanced chemiluminescence assay.

Akt kinase activity in Aβ-treated microglia was measured with the Cell Signaling nonradioactive Akt kinase assay kit. Microglia lysates were immunoprecipitated with the anti-Akt1 antibody. Immunoprecipitates were washed three times with lysis buffer and twice with Akt kinase buffer containing 20 mM HEPES (pH 7.4), 10 mM $MgCl_2$, 10 mM $MnCl_2$. Kinase assays were performed for 30 min at 30°C under continuous agitation in kinase buffer containing 200 μM ATP, 1 μg of GSK-3 fusion protein, according to the manufacturer's instructions. Phosphorylation of GSK-3 was analysed by Western blot using anti-phospho-GSK-3$\alpha\beta$ antibody.

Statistical analysis

Each experiment was performed at least three times and the results were presented as mean ± S.E.M. The data were analysed by one-way analysis of variance (ANOVA). A level of $P < 0.05$ was considered significant.

Results

Aβ-induced assembly of NADPH oxidase and the consequent production of ROS might play a central role in oxidative stress-related neuronal injury in AD models; accordingly, antioxidants, including melatonin, might

protect neurons via eliminating the microglia-derived ROS. To test this possibility, cultures of microglia were incubated in the presence of fibrillar Aβ doses ranging between 5 and 20 μM. Fig. 1A illustrates that fibrillar Aβ induced a dose- and time-dependent increase of ROS production, as indicated by the increase in cellular DCF fluorescence. Incubation of microglia with 20 μM Aβ for 6 hr increased the cellular ROS by 7.3-fold as compared with that measured in unstimulated microglia.

To ascertain if the increase in cellular ROS level was because of the assembly and the activation of NADPH oxidase, microglia were pretreated with NADPH oxidase inhibitor DCI, or superoxide anion scavenger MnTMPyP. In microglia pretreated with DCI (5 μM) or MnTMPyP (25 μM), Aβ-induced increase in cellular ROS level was complete abolished (Fig. 1B). Furthermore, the generation of superoxide anion by NADPH oxidase was detected in microglia activated by fibrillar Aβ. As shown in Fig. 1C, a typical EPR spectrum of DMPO-O_2^- spin adduct could be observed in microglia activated by fibrillar Aβ, suggesting the generation of superoxide anion. Taken the above data together, the Aβ induced microglia ROS production in an associated manner to the activation of microglial NADPH oxidase.

The effects of melatonin on ROS production in Aβ-activated microglia were measured. Pretreating microglia with melatonin dose-dependently decreased the cellular ROS level, as shown in Fig. 2A. In microglia pretreated with 100 μM of melatonin, Aβ-induced increase in cellular ROS level was complete abolished.

To confirm whether melatonin decreased the cellular ROS level by inhibiting the activity of NADPH oxidase or by scavenging the superoxide anion directly, melatonin was added to microglia preactivated with Aβ, which generate high levels of ROS via activated NADPH oxidase, and the changes in cellular ROS level were measured. Interestingly, melatonin (up to 100 μM) shows no significant effects on ROS generation in microglia preactivated with Aβ (Fig. 2B), suggesting that melatonin could not inhibit the activity of NADPH oxidase and could not scavenge the superoxide anion directly.

The direct scavenging of superoxide anion by melatonin was further studied by EPR spectrometry in a hypoxanthine/xanthine oxidase system. However, no apparent direct superoxide-scavenging capacity could be observed in reaction mixture containing 100 μM melatonin. Melatonin only shows significant superoxide-scavenging capacity at 250 μM (Fig. 2C).

Taken the above data together, the decrease in cellular ROS level in melatonin-pretreated microglia was because of the inhibition of ROS production, rather than the direct scavenging of ROS. Melatonin inhibits the activation of NADPH oxidase in Aβ-stimulated microglia, but shows no apparent inhibition effect on activated NADPH oxidase.

The translocation of $p47^{phox}$ and $p67^{phox}$ subunits of NADPH oxidase from the cytosol to the plasma membrane is an essential step for the activation of NADPH oxidase. In order to elucidate the effect of melatonin on NADPH oxidase activation, membrane levels of $p47^{phox}$ and $p67^{phox}$ were evaluated in microglia pretreated with melatonin and stimulated with Aβ. Fig. 3A illustrates that Aβ stimulation

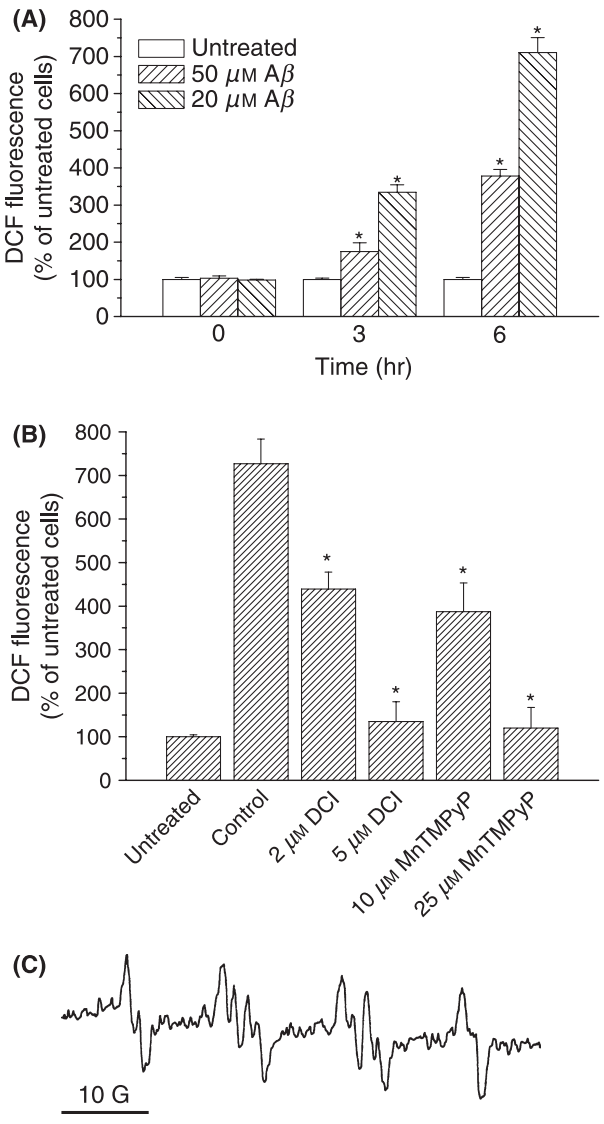

Fig. 1. Production of superoxide anion in fibrillar Aβ-activated microglia. (A) Dose- and time-dependent increase in cellular DCF fluorescence in microglia exposed to fibrillar Aβ. Microglia grown on 96-well microplate were exposed to Aβ (5 or 20 μM) for 0, 3 or 6 hr, respectively, loaded with 20 μM DCFH-DA, and incubated for additional 1 hr. The fluorescent signal of DCF was detected with Fluoroskan Ascent microplate reader with excitation wavelength 485 nm and emission wavelength 538 nm. Data are mean ± S.E.M. of eight samples. $^*P < 0.01$ in comparison with untreated cells. (B) Inhibition of NADPH oxidase activity by DCI or scavenging of superoxide anion by MnTMPyP significantly decreased the cellular DCF fluorescence. Microglia grown on 96-well microplate were pretreated with the NADPH oxidase inhibitor DPI (2 or 5 μM) or superoxide anion scavenger MnTMPyP (10 or 25 μM) for 30 min and then exposed to 20 μM Aβ for 6 hr. After loading with 20 μM DCFH-DA for 1 hr, the fluorescent signal of DCF was detected. Data are mean ± S.E.M. of eight samples. $^*P < 0.01$ in comparison with control cells. (C) Typical ESR spectrum of DMPO-O_2^- spin adduct observed in fibrillar Aβ-activated microglia. Microglia were exposed to Aβ for 6 hr and suspended in 100 μL of HBSS containing 0.1 M of the spin trap DMPO. After incubation at 37°C for 2 min, the EPR spectrum was recorded immediately with a Bruker ER-200 D-SRC EPR spectrometer.

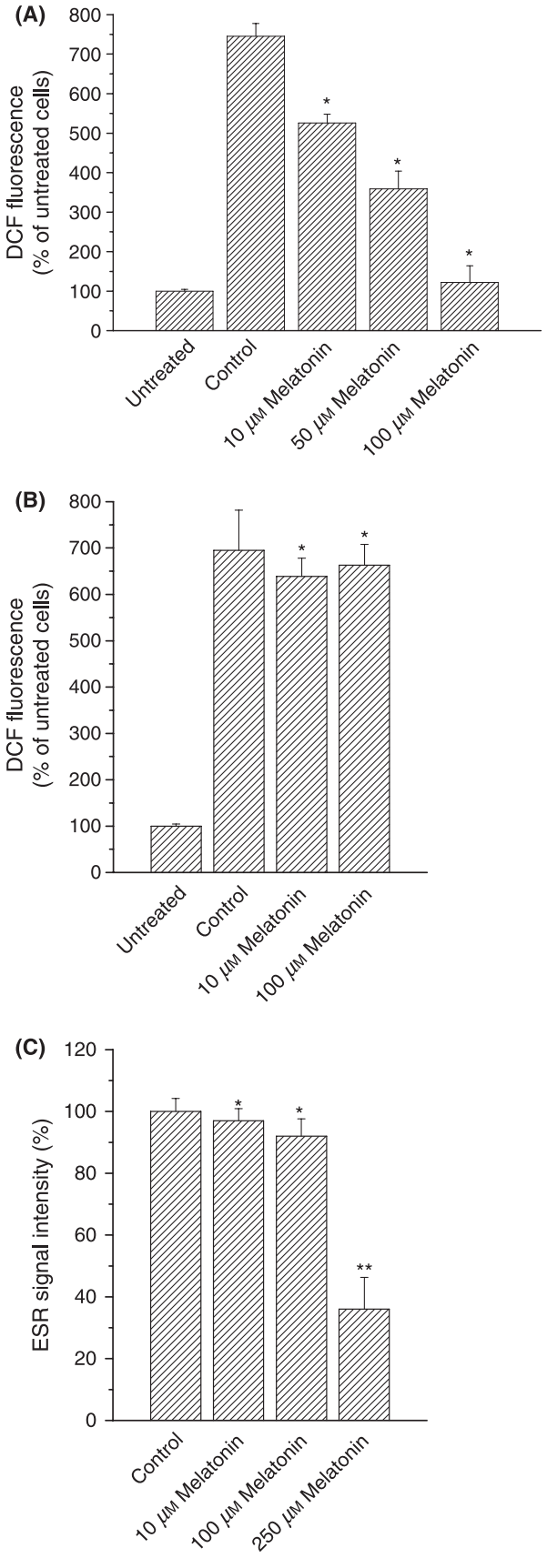

Fig. 2. Melatonin inhibits the production of superoxide anion in fibrillar Aβ-activated microglia. (A) Pretreating microglia with melatonin dose-dependently decreased the the production of superoxide anion. Microglia grown on 96-well microplate were pretreated with melatonin (10, 50 or 100 μM) for 30 min and then exposed to 20 μM Aβ for 6 hr. The production of superoxide-derived ROS was detected with DCFH-DA. Data are mean ± S.E.M. of eight samples. $^{*}P < 0.01$ in comparison with control cells. (B) Melatonin shows no inhibition effects on activated NADPH oxidase. Microglia grown on 96-well microplate were exposed to 20 μM Aβ for 6 hr to activate the NADPH oxidase and then incubated with melatonin (10 or 100 μM) for 30 min. The production of superoxide-derived ROS was detected with DCFH-DA. Data are mean ± S.E.M. of eight samples. $^{*}P > 0.05$ in comparison with control cells. (C) Melatonin scavenges superoxide anion generated by hypoxanthine/xanthine oxidase system at high concentration. Reaction mixtures contained 0.5 mM hypoxanthine, 0.96 mM DETAPAC, 0.1 M DMPO, 0.05 U/mL xanthine oxidase and different concentrations of melatonin. The ESR spectra were recorded 40 s after the addition of xanthine oxidase. $^{*}P > 0.05$ in comparison with control. $^{**}P < 0.01$ in comparison with control.

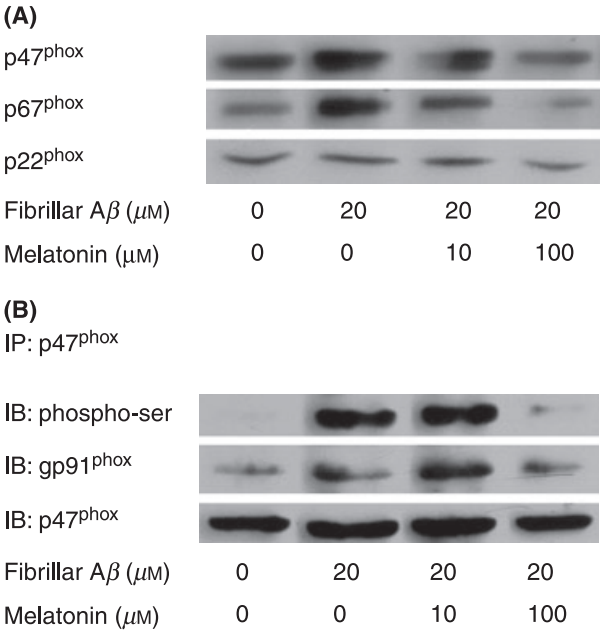

Fig. 3. Melatonin impairs the assembly of NADPH oxidase. (A) Melatonin inhibits the translocation of $p47^{phox}$ and $p67^{phox}$ subunits of NADPH oxidase from the cytosol to the plasma membrane. Microglia were pretreated with or without melatonin for 30 min and then exposed to Aβ for 1 hr and the translocation of $p47^{phox}$ and $p67^{phox}$ subunits to the plasma membrane was measured by Western blot. The membrane levels of the $p22^{phox}$ subunit were monitored as a control. (B) Melatonin inhibits the phosphorylation of $p47^{phox}$ and down regulates the binding of $p47^{phox}$ to $gp91^{phox}$. Microglia were pretreated with or without melatonin for 30 min and then exposed to Aβ for 1 hr. The $p47^{phox}$ was immunoprecipitated, the phosphorylation of $p47^{phox}$ and the binding of $p47^{phox}$ to $gp91^{phox}$ was analysed by Western blot.

enhanced translocation of both $p47^{phox}$ and $p67^{phox}$ subunits to the plasma membrane. After incubation with Aβ for 1 hr, both $p47^{phox}$ and $p67^{phox}$ levels in the plasma

membrane increased significantly. The membrane levels of $p22^{phox}$, in keeping with it being an integral membrane protein, were similar in proportions from both untreated and Aβ-treated microglia.

Pretreatment of microglia with 100 μM melatonin significantly decreased the Aβ-induced mobilization of $p47^{phox}$ and $p67^{phox}$ subunits to plasma membrane, suggesting that melatonin impairs the assembly of NADPH oxidase.

The translocation of $p47^{phox}$ is triggered by its phosphorylation, which induces a conformational change that mediates the interaction with both $gp91^{phox}$ and $p67^{phox}$. To ascertain whether melatonin decreased the Aβ-induced mobilization of $p47^{phox}$ to plasma membrane by modulating its phosphorylation, the effects of melatonin on $p47^{phox}$ phosphorylation were studied by immunoprecipitation. Melatonin significantly decreased the phosphorylation of the serine residues of $p47^{phox}$ and impairs the binding of $p47^{phox}$ to $gp91^{phox}$, as shown in Fig. 3B. This result indicated that the inhibition of NADPH oxidase assembly by melatonin was related to modulating the phosphorylation of $p47^{phox}$.

The production of cellular ROS could be inhibited by the PI3K inhibitors, wortmannin and LY294002 (Fig. 4A). Also, Aβ-induced $p47^{phox}$ phosphorylation in microglia could be abolished by wortmannin and LY294002 (Fig. 4B). These results showed that PI3K was involved in $p47^{phox}$ phosphorylation and the subsequent NADPH oxidase assembly during the activation of Aβ-stimulated microglia.

As it is widely accepted that Akt is the Ser/Thr kinase in the downstream of PI3K, we examined whether the Akt was responsible for $p47^{phox}$ phosphorylation and participated in NADPH oxidase activation. Phosphorylation of Akt after Aβ stimulation was assessed to determine whether Aβ could activate Akt in microglia. As shown in Fig. 5A, Akt phosphorylation was evident at 30 min after Aβ-stimulation and this Akt activation was completely abolished by PI3K inhibitors, demonstrating that Akt activation was evoked by Aβ as a downstream event of PI3K activation. Inhibition of Akt by its inhibitor 1L-6-hydroxymethyl-chiro-inositol 2-(R)-2-O-methyl-3-O-octadecylcarbonate significantly decreased the production of ROS (Fig. 5B) and induced a marked decrease in the $p47^{phox}$ phosphorylation levels (Fig. 5C), suggesting that Akt is the key mediator of $p47^{phox}$ phosphorylation and NADPH oxidase assembly.

The Akt activity in microglia pretreated with melatonin was assayed. Fig. 6 shows that melatonin inhibits the activity of Akt dose dependently. In microglia pretreated with 100 μM melatonin and then exposed to Aβ, no apparent phospho-GSK-3 (Akt substrate) could be detected.

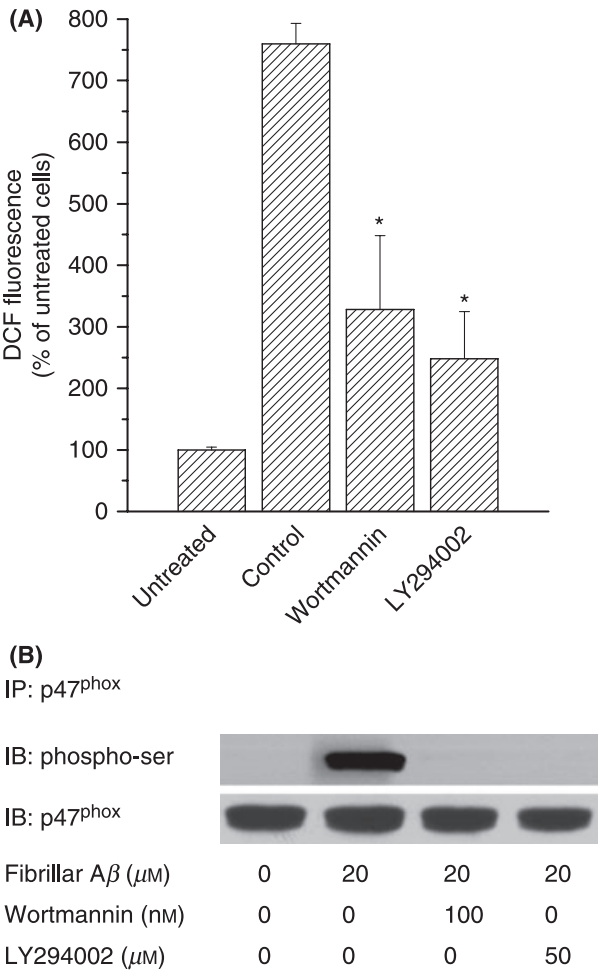

Fig. 4. Involvement of PI3K signalling pathway in Aβ-induced NADPH oxidase assembly. (A) Inhibition of PI3K decreases the production of superoxide anion in fibrillar Aβ-activated microglia. Microglia grown on 96-well microplate were pretreated with the PI3K inhibitors wortmannin (100 nM) or LY294002 (50 μM) for 30 min and then exposed to 20 μM Aβ for 6 hr. The production of superoxide-derived ROS was detected with DCFH-DA. Data are mean ± S.E.M. of eight samples. $*P < 0.01$ in comparison with control cells. (B) Inhibition of PI3K abolishes the phosphorylation of $p47^{phox}$ in Aβ-activated microglia. Microglia were pretreated with the PI3K inhibitors wortmannin (100 nM) or LY294002 (50 μM) for 30 min and then exposed to 20 μM Aβ for 1 hr. The phosphorylation of $p47^{phox}$ was analysed by Western blot.

Discussion

In spite of a large number of studies undertaken, the aetiology of AD is largely unknown. Many mechanisms have been proposed, including genetic predispositions, inflammatory processes associated with cytokine release, oxidative stress and neurotoxicity by metal ions [27]. Recently, much attention has been paid to microglial activation as a major pathogenic factor for AD [28, 29]. The senile plaques (plaques of Aβ) are surrounded by degenerating neurons and activated microglia; and the latter cells are largely responsible for the proinflammatory environment within the diseased brain. Microglial activation has been reported to be a relatively early pathogenetic event which precedes the process of neuronal destruction in AD patients [30]. In response to contact with fibrillar Aβ, microglia secrete a diverse array of proinflammatory molecules such as proinflammatory cytokines (e.g. tumour necrosis factor-α, interleukin-1β), ROS and reactive nitrogen species.

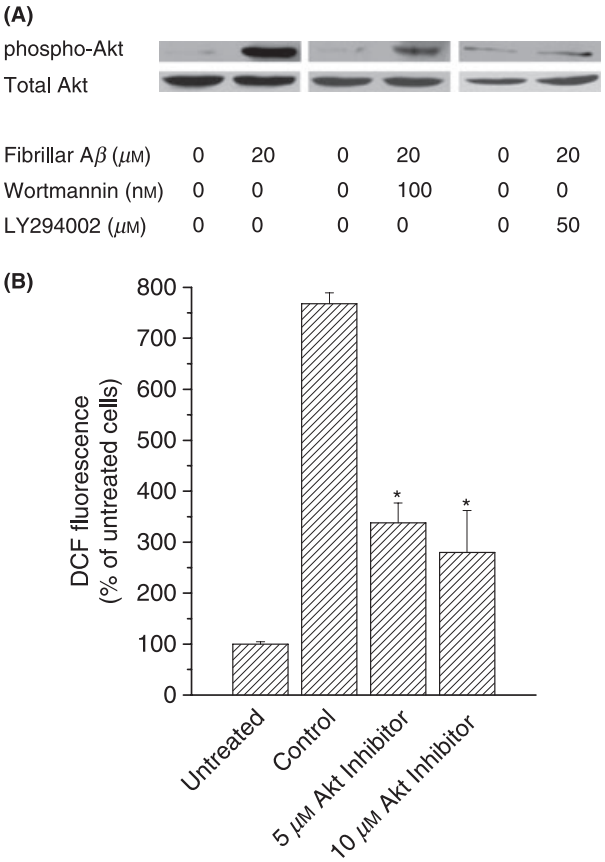

Fig. 5. Involvement of Akt signalling pathway in Aβ-induced NADPH oxidase assembly. (A) Fibrillar Aβ activates the microglial Akt phosphorylation in a PI3K-dependent manner. Microglia were pretreated with the PI3K inhibitors wortmannin (100 nM) or LY294002 (50 μM) for 30 min and then exposed to 20 μM Aβ for 30 hr. The phosphorylation of Akt was analysed by Western blot. (B) Inhibition of Akt decreases the production of superoxide anion in fibrillar Aβ-activated microglia. Microglia grown on 96-well microplate were pretreated with the Akt inhibitor 1L-6-hydroxymethyl-chiro-inositol 2-(R)-2-O-methyl-3-O-octadecylcarbonate (5 and 10 μM) for 30 min and then exposed to 20 μM Aβ for 6 hr. The production of superoxide-derived ROS was detected with DCFH-DA. Data are mean ± S.E.M. of eight samples. $*P < 0.01$ in comparison with control cells. (C) Inhibition of Akt abolishes the phosphorylation of $p47^{phox}$ in Aβ-activated microglia. Microglia were pretreated with the Akt inhibitor (5 and 10 μM) for 30 min and then exposed to 20 μM Aβ for 1 hr. The phosphorylation of $p47^{phox}$ was analysed by Western blot.

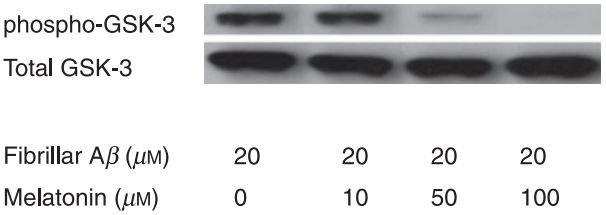

Fig. 6. Melatonin inhibits Akt activation in fibrillar Aβ-activated microglia. Microglia were pretreated with or without melatonin for 30 min and then exposed to Aβ for 30 min. The Akt kinase activity in Aβ-treated microglia was measured with the Cell Signaling nonradioactive Akt kinase assay kit. Phosphorylation level of GSK-3 was used as a maker of Akt activity.

Oxidative stress plays a crucial role in the pathogenesis of AD [24], and microglia have been postulated to be a potential source of oxidative stress in response to Aβ peptides in the AD brain. In response to contact with fibrillar Aβ, microglia generate ROS by the phagocytic NADPH oxidase. NADPH oxidase plays an essential role in innate immunity by catalyzing the formation of superoxide and superoxide-derived ROS (including hydrogen peroxide, hydroxyl radicals and peroxynitrite), which facilitates the destruction of pathogens. The excessive production of ROS can damage neurons adjacent to the sites of inflammatory action, thereafter, the activation of the NADPH oxidase must be tightly controlled through regulated assembly of the individual oxidase subunits into a functionally active complex.

Melatonin and its metabolites scavenge superoxide anions and superoxide-derived ROS directly [6–9]. Melatonin also shows significant protective effects against Aβ-induced oxidative stress in AD models [12–14], and it is hypothesized that the protective effects of melatonin and its derivatives are related to its antioxidant properties. However, the regulatory effects of melatonin on NADPH oxidase assembly remain unclear. In the present investigation, we provided direct evidence that melatonin could impair the assembly of NADPH oxidase in Aβ-activated microglia and inhibit the generation of ROS in a dose-dependent manner.

The mechanism of Aβ-induced assembly of NADPH oxidase in microglia has been reviewed elsewhere [21]. Microglial contact with fibrillar Aβ catalyses the assembly of an ensemble of cell surface receptors that includes CD36, α6β1 integrin, CD47 and the class A scavenger receptor. Fibrillar Aβ engagement of this receptor complex leads to the initiation of complex signalling events leading to the activation of kinases Lyn, Fyn, Syk and PI3K, which are responsible for activating NADPH oxidase assembly. The NADPH oxidase consists of two integral membrane proteins, $p22^{phox}$ and $gp91^{phox}$, which together form a heterodimeric flavoprotein known as cytochrome b_{558}. In addition, there are four regulatory components $p47^{phox}$, $p67^{phox}$, $p40^{phox}$ and the small G-protein Rac reside in the cytosol of the resting cells. Activation of multiple kinases Lyn, Fyn, Syk and PI3K by Aβ leading to the phosphorylation of $p47^{phox}$ and $p67^{phox}$, and the GDP/GTP exchange on Rac. The cytosolic components then translocate to the membrane to assemble an activated NADPH oxidase complex, which initiates electron flow and generation of superoxide through the NADPH-derived electron reduction by the flavocytochrome.

In the present investigation, we found that inhibition of microglial PI3K significantly inhibits ROS production, suggesting the involvement of PI3K in NADPH oxidase assembly directly or indirectly. NADPH oxidase activation critically depends on $p47^{phox}$ phosphorylation [31]. p38 MAPK, ERK1/2, protein kinase C and Akt have been suggested as activators of $p47^{phox}$ phosphorylation in response to proinflammatory stimuli. Our data suggested that PI3K regulates $p47^{phox}$ phosphorylation via an Akt-dependent pathway. Inhibition of PI3K down-regulated the activity Akt and decreased the phosphorylation of $p47^{phox}$. Interestingly, pretreatment of microglia with melatonin significantly decreased the Akt activation. Recently, the molecular mechanisms of melatonin's protection effects have been widely investigated. Killic et al. reported [32] that acute melatonin treatment could activate the neuroprotective PI3K/Akt signalling pathway in an ischaemic brain injury model; however, prophylactic melatonin treatment activated the ERK and/or JNK MAPKs rather than the PI3K/Akt signalling pathway in the same ischaemic brain injury model. Martin et al. reported [33] that melatonin could inhibit the Akt activation in C6 glioma cells. In our experimental model, melatonin impairs the fibrillar Aβ-induced assembly of the NADPH oxidase and significantly inhibits the production of superoxide anion-derived ROS via a PI3K/Akt related mechanism.

Considerable attention has been devoted to melatonin as a potential therapeutic intervention in AD. It is believed that melatonin reduces oxidative stress by scavenging free radicals. However, previous studies have not directly analysed the relationship between melatonin and fibrillar Aβ-dependent activation of the NADPH oxidase. Our data offer new insights into the mechanism of inhibiting ROS generation by melatonin in Aβ-activated microglia. Inhibition of ROS production indirectly might be the underlying mechanism for the neuroprotection by melatonin in the AD brain.

Acknowledgements

This work was supported by grants from the National Natural Science Foundation of China (Grants 30670480 and 30770492) and the National Basic Research Program of China (Grants 2004CB720000, 2006CB705600 and 2006CB911001).

References

1. Reiter RJ. Pineal melatonin: cell biology of its synthesis and of its physiological interactions. Endocr Rev 1991; **12**:151–180.
2. Tan DX, Manchester LC, Reiter RJ et al. Identification of highly elevated levels of melatonin in bone marrow: its origin and significance. Biochim Biophys Acta 1999; **1472**:206–214.
3. Arendt J. Melatonin, circadian rhythms and sleep. New Engl J Med 2000; **343**:1114–1116.
4. Tricoire H, Locatelli A, Chemineau P et al. Melatonin enters the cerebrospinal fluid through the pineal recess. Endocrinology 2002; **143**:84–90.
5. Reiter RJ, Tan DX. Role of CSF in the transport of melatonin. J Pineal Res 2002; **33**:61.
6. Reiter RJ, Tan DX, Manchester LC et al. Biochemical reactivity of melatonin with reactive oxygen and nitrogen species: a review of the evidence. Cell Biochem Biophys 2001; **34**:237–256.
7. Allegra M, Reiter RJ, Tan DX et al. The chemistry of melatonin's interaction with reactive species. J Pineal Res 2003; **34**:1–10.
8. Tan DX, Manchester LC, Terron MP et al. One molecule, many derivatives: a never-ending interaction of melatonin with reactive oxygen and nitrogen species? J Pineal Res 2007; **42**:28–42.
9. Hardeland R, Backhaus C, Fadavi A. Reactions of the NO redox forms NO^+, $^{\bullet}NO$ and HNO (protonated NO^-) with the melatonin metabolite N^1-acetyl-5-methoxykynuramine. J Pineal Res 2007; **43**:382–388.
10. Mayo JC, Tan DX, Sainz RM et al. Protection against oxidative protein damage induced by metal-catalyzed reaction or alkylperoxyl radicals: comparative effects of melatonin and other antioxidants. Biochim Biophys Acta 2003; **1620**:139–150.
11. Manda K, Ueno M, Anzai K. AFMK, a melatonin metabolite, attenuates X-ray-induced oxidative damage to DNA, proteins and lipids in mice. J Pineal Res 2007; **42**:386–393.
12. Rosales-Corral S, Tan DX, Reiter RJ et al. Orally administered melatonin reduces oxidative stress and proinflammatory cytokines induced by amyloid-β peptide in rat brain: a comparative, *in vivo* study versus vitamin C and E. J Pineal Res 2003; **35**:80–84.
13. Lahiri DK, Chen DM, Lahiri P et al. Amyloid, cholinesterase, melatonin, and metals and their roles in aging and neurodegenerative diseases. Ann N Y Acad Sci 2005; **1056**:430–449.
14. Srinivasan V, Pandi-Perumal SR, Cardinali DP et al. Melatonin in Alzheimer's disease and other neurodegenerative disorders. Behav Brain Funct 2006; **2**:15.
15. Mayo JC, Sainz RM, Tan DX et al. Melatonin and Parkinson's disease. Endocrine 2005; **27**:169–178.
16. Sharma R, McMillan CR, Tenn CC et al. Physiological neuroprotection by melatonin in a 6-hydroxydopamine model of Parkinson's disease. Brain Res 2006; **1068**:230–236.
17. Chen HY, Chen TY, Lee MY et al. Melatonin decreases neurovascular oxidative/nitrosative damage and protects against early increases in the blood-brain barrier permeability after transient focal cerebral ischemia in mice. J Pineal Res 2006; **41**:175–182.
18. Selkoe DJ. Alzheimer's disease: genes, proteins, and therapy. Physiol Rev 2001; **81**:741–766.
19. Selkoe DJ. Cell biology of protein misfolding: the examples of Alzheimer's and Parkinson's disease. Nat Cell Biol 2004; **6**:1054–1061.
20. Gandy S. The role of cerebral amyloid-β accumulation in common forms of Alzheimer disease. J Clin Invest 2005; **115**:1121–1129.
21. Wilkinson BL, Landreth GE. The microglial NADPH oxidase complex as a source of oxidative stress in Alzheimer's disease. J Neuroinflammation 2006; **3**:30.
22. Wei T, Zhao X, Hou J et al. The antioxidant ESeroS-GS inhibits NO production and prevents oxidative stress in astrocytes. Biochem Pharmacol 2003; **66**:83–91.
23. Wei T, Chen C, Hou J et al. Nitric oxide induces oxidative stress and apoptosis in neuronal cells. Biochim Biophys Acta 2000; **1498**:72–79.
24. Zhang Z, Wei T, Hou J et al. Tetramethylpyrazine scavenges superoxide anion and decreases nitric oxide production in

human polymorphonuclear leukocytes. Life Sci 2003; **72**:2465–2472.
25. Wei T, Chen C, Li F et al. Antioxidant properties of EPC-K1: a study on mechanisms. Biophys Chem 1999; **77**:153–160.
26. Alvarez-Maqueda M, El Bekay R, Monteseirin J et al. Homocysteine enhances superoxide anion release and NADPH oxidase assembly by human neutrophils. Effects on MAPK activation and neutrophil migration. Atherosclerosis 2004; **172**:229–238.
27. Butterfield DA, Reed T, Newman SF et al. Roles of amyloid beta-peptide-associated oxidative stress and brain protein modifications in the pathogenesis of Alzheimer's disease and mild cognitive impairment. Free Radic Biol Med 2007; **43**:658–677.
28. Simard AR, Soulet D, Gowing G et al. Bone marrow-derived microglia play a critical role in restricting senile plaque formation in Alzheimer's disease. Neuron 2006; **49**:489–502.
29. Heneka MT, O'Banion MK. Inflammatory processes in Alzheimer's disease. J Neuroimmunol 2007; **184**:69–91.
30. Sastre M, Klockgether T, Heneka MT. Contribution of inflammatory processes to Alzheimer's disease: molecular mechanisms. Int J Dev Neurosci 2006; **24**:167–176.
31. Perisic O, Wilson MI, Karathanassis D et al. The role of phosphoinositides and phosphorylation in regulation of NADPH oxidase. Adv Enzyme Regul 2004; **44**:279–298.
32. Kilic U, Kilic E, Reiter RJ et al. Signal transduction pathways involved in melatonin-induced neuroprotection after focal cerebral ischemia in mice. J Pineal Res 2005; **38**:67–71.
33. Martin V, Herrera F, Garcia-Santos G et al. Involvement of protein kinase C in melatonin's oncostatic effect in C6 glioma cells. J Pineal Res 2007; **43**:239–244.